Original Articles

Acupuncture and Herbal Medicine

Astragalus injection alleviates diabetic cognitive impairment (DCI) through dual effects of anti-neuroinflammation and antioxidative stress based on network pharmacology analysis and experimental validation

Tong Xia[1], Fayin Huang[2], Shiqi Li[2], Yijing Yan[2], Lin Guo[1], Wenlan Zhang[1], Yulin Wang[2], Peizhe Lin[3], Yijing Wang[4], Yanrong Suo[5], Maojuan Guo[1], Xijuan Jiang[1], Huhu Li[1,*], Yongna Dai[2,*], Wenyun Zeng[6,*]

[1]School of Integrative Medicine, Tianjin University of Traditional Chinese Medicine, Tianjin, China; [2]School of Traditional Chinese Medicine, Tianjin University of Traditional Chinese Medicine, Tianjin, China; [3]Guang'anmen Hospital, China Academy of Chinese Medical Sciences, Beijing, China; [4]School of Acupuncture & Moxibustion and Tuina, Tianjin University of Traditional Chinese Medicine, Tianjin, China; [5]Traditional Chinese Medicine Department, Ganzhou People's Hospital, Ganzhou, China; [6]Oncology Department, Ganzhou People's Hospital, Ganzhou, China

Abstract

Objective: To explore the effects of astragalus injection (AI) in patients with diabetic cognitive impairment (DCI).

Methods: First, to screen for effective chemical components of astragalus, we searched Traditional Chinese Medicines Systems Pharmacology (TCMSP) and Analysis Platform databases. We then predicted the corresponding potential target genes using Swiss Target Prediction, searched and filtered three disease databases to identify DCI targets, and constructed a drug-component-target-disease interaction network and protein–protein interaction (PPI) network. The core targets and pathways of AI against DCI were predicted using Gene Ontology (GO) and Kyoto Encyclopedia of Genes and Genomes (KEGG) functional enrichment analyses. *In vivo* experiments demonstrated the efficacy of AI in alleviating diabetes-associated cognitive impairment, whereas *in vitro* studies verified its anti-inflammatory and antioxidant stress mechanisms. Finally, western blot analysis identified key regulatory proteins involved in inflammation and oxidative stress, proposing a potential mechanism by which AI mitigates DCI through modulation of these proteins.

Results: We screened 25 active components of astragalus and 251 drug targets and obtained 220 common targets after intersecting 8,036 DCI targets. GO enrichment analysis showed that astragalus mainly treats DCI by regulating the response to external stimuli, lipopolysaccharide, hypoxia, and oxygen levels. KEGG pathway enrichment analysis revealed that it was mainly involved in cancer, calcium signaling, p53 signaling, vascular endothelial growth factor (VEGF) signaling pathway, and Toll-like receptor (TLR) signaling pathways. Experimental results demonstrated that AI alleviates diabetes-associated cognitive impairment through dual mechanisms: activating the Kelch-like ECH-associated protein (Keap1)/nuclear factor-erythroid-derived related factor 2 (Nrf2) signaling pathway to exert antioxidant effects, and inhibiting the TLR-4/nuclear factor-kappa B (NF-κB) signaling pathway to mitigate neuroinflammation, thereby improving cognitive dysfunction and hyperglycemia.

Conclusions: Network pharmacology identified potential AI interventions for DCI, and experiments were conducted to confirm some of the major targets in the predictive signaling pathway. Our study offers new insights into the mechanisms of AI treatment for DCI.

Keywords: Astragalus injection, Astragalus membranaceus Cognitive impairment of diabetes, anti-neuroinflammation, antioxidative stress, Network pharmacology

Graphical Abstract: https://links.lww.com/AHM/A205

Tong Xia, Fayin Huang, and Shiqi Li contributed equally to this work.

**Corresponding author. Huhu Li, E-mail: woshihuhu163@163.com; Yongna Dai, E-mail: daiyongna@foxmail.com; Wenyun Zeng, E-mail: 605422923@qq.com.*

How to cite this article: *Xia T, Huang FY, Li SQ, Yan YJ, Guo L, Zhang WL, Wang YL, Lin PZ, Wang YJ, Suo YR, Guo MJ, Jiang XJ, Li HH, Dai YN, Zeng WY. Astragalus injection alleviates diabetic cognitive impairment (DCI) through dual effects of anti-neuroinflammation and antioxidative stress based on network pharmacology analysis and experimental validation. Acupunct Herb Med 2026;6(2):230–246. doi: 10.1097/HM9.0000000000000185*

Received 02 January 2025 / Accepted 23 January 2026

Copyright © 2026 Tianjin University of Traditional Chinese Medicine. This is an open-access article distributed under the terms of the Creative Commons Attribution-Non Commercial-No Derivatives License 4.0 (CCBY-NC-ND), where it is permissible to download and share the work provided it is properly cited. The work cannot be changed in any way or used commercially without permission from the journal.

HM9_V6N2.indb 230 25-Jun-26 00:45:10

Introduction

Type 1 diabetes mellitus (T1DM), one of the most prevalent chronic autoimmune diseases, typically manifests in pediatric and adolescent populations. Globally, approximately 500,000 individuals are diagnosed with T1DM, representing 10% of all cases[1]. T1DM, also known as insulin-dependent diabetes mellitus (IDDM), is characterized by insulin deficiency and is commonly treated with various forms of exogenous insulin (rapid-acting, short-acting, intermediate-acting, and long-acting)[2]. Notably, microvascular dysfunction and neuronal impairment within the central nervous system resulting from diabetes, referred to as diabetic cognitive impairment (DCI), are significant complications of various types of diabetes[3]. Persistent hyperglycemia significantly increases the risk of cognitive impairment, which may progress to dementia[4–6]. Numerous studies have demonstrated that individuals with T1DM, both children and adults, exhibit diverse levels of cognitive dysfunction, primarily characterized by deficits in cognitive flexibility, attention, psychomotor speed, learning, and memory, which tend to worsen over time[3,7]. The incidence of T1DM is increasing worldwide. However, efficacious and definitive treatment modalities are lacking. Consequently, exploring the precise pathogenesis of T1DM and its associated complications, as well as developing effective therapeutic interventions, is imperative.

Traditional Chinese medicine has a wealth of experience and distinctive advantages in the treatment of diabetes[8–9]. Astragalus injection (AI) is effective in treating a range of systemic ailments, including weakness, wounds, anemia, fever, multiple allergies, chronic fatigue, loss of appetite, uterine bleeding, and uterine prolapse, and also plays a crucial role in preventing diabetes and its complications, including nephropathy, cardiomyopathy, and retinopathy[10–12]. Numerous studies have indicated that AI exhibits a wide array of functions, including immune regulation, anti-hyperglycemia, anti-inflammation, anti-oxidation, and antiviral activities. Specifically, the protective effect of AI against neurological disorders in the presence of diabetes has been extensively validated, possibly due to its ability to attenuate neuroinflammatory processes and mitigate oxidative stress triggered by hyperglycemia[13–14]. Several studies have used AI as a therapeutic intervention to manage diabetes and its associated complications. Nevertheless, additional research is required to establish its effectiveness and pharmacological effects on DCI.

Network pharmacology is an interdisciplinary field integrating systems biology and network informatics. In recent years, this method has been extensively used in the development of novel medications and offers significant benefits in understanding the pharmacological mechanisms of traditional Chinese medicine with multiple components, targets, and pathways[15]. Consequently, in this study, we utilized network pharmacology to screen the intersection target of AI and DCI, identified the important research pathways, and further confirmed that AI played both antioxidative stress and anti-neuroinflammation effects by regulating Kelch-like ECH-associated protein (Keap1)/nuclear factor-erythroid-derived–related Factor 2 (Nrf2) pathway and TLR-4/nuclear factor-kappa B (NF-κB) pathway to treat DCI rats through animal experiments.

Materials and methods

Chemicals and reagents

AI was provided by Shijiazhuang Shineway Pharmaceutical Co., Ltd. (Hebei, China; Z13020999). Streptozotocin (STZ) was purchased from Sigma-Aldrich Corporation (St. Louis, MO, USA; S0130). Saline–sodium Citrate (SSC) Buffer and lipopolysaccharide (LPS) were purchased from Beijing Solarbio Technology Co., Ltd. (Beijing, China; S8050; C1013; L8880). A glucose oxidase peroxidase diagnostic enzyme kit was purchased from Shanghai Rongsheng Biotech Co., Ltd. (Shanghai, China; CAT361500). Tumor necrosis factor-α (TNF-α), interleukin (IL) 1β, and IL-10 enzyme-linked immunosorbent assay (ELISA) kits were purchased from Wuhan Uscn Sciences Co., Ltd. (Wuhan, China; SEA133Ra, SEA563Ra, SEA056Ra). Superoxide dismutase (SOD) Colorimetric Assay Kit (E-BC-K020-M) and malondialdehyde (MDA) colorimetric assay kits (E-BC-K028-M) were purchased from Elabscience Biotechnology Co., Ltd. (Wuhan, China). A hydrogen peroxide solution (DGH_2O_2) was obtained from Dingguo Changsheng Biotechnology (Beijing, China). The Cell Counting Kit-8 (CCK-8) (GK10005) was acquired from GLPBIO (Montclair, CA, USA). The DMEM-H Liquid Medium (C11995500BT) was obtained from Gibco (Thermo Fisher Scientific, Waltham, MA, USA).

Animals and experimental grouping

Animals feeding

Specific pathogen-free (SPF) male Wistar rats (8 weeks old, weight 220 ± 20 g) were purchased from Beijing Vital River Laboratory Animal Technology Co., Ltd. (Certificate No.: SCXK (JING) 2021-0006). All the animals were housed in the SPF animal room of the Animal Center of Tianjin University of Traditional Chinese Medicine and had ad libitum access to food and water in a 12-hour light/dark cycle (temperature 22 ± 2°C, humidity 50 ± 10%). All animal experiments were approved by the Ethics Committee of the Tianjin University of Traditional Chinese Medicine (Animal Experiment Ethics No.: TCM-LAEC2023267X1634), and all laboratory procedures were performed according to the principles outlined in the National Institutes of Health (NIH) Guide for the Care and Use of Laboratory Animals.

Model replication

Following adaptive feeding for 1 week, the Morris Water Maze (MWM) experiment was performed to remove rats with cognitive impairments. Rats with normal cognitive function were randomly divided into control and model groups. The model group rats were intraperitoneally injected with STZ dissolved in SSC (60 mg/kg)[16] for 3 consecutive days. After 72 hours of the last injection of STZ, the fasting blood glucose

HM9_V6N2.indb 231 25-Jun-26 00:45:10

(FBG) in the tail vein of the rats was measured using a blood glucose meter (URIT-80; URIT MEDICAL Electronic Co., Ltd., Guilin, China). Rats with FBG ≥11.1 mmol/L were considered successfully modeled for T1DM. In the control group, the rats received the same volume of SSC solution for three consecutive days. Having successfully replicated the T1DM model, the rats were fed a normal diet for 10 weeks in both the control and model groups. After 10 weeks, behavioral changes in each group were detected using an MWM test to evaluate cognitive impairment.

Experimental design

The model group rats were randomly divided into four groups: DCI, DCI + low-dose AI group (AI-L), DCI + medium-dose AI group (AI-M), and DCI + high-dose AI group (AI-H). Owing to mortality in the experiment, the final control group and four intervention groups had an average of six rats each. Based on a comprehensive literature review, the administered dose in rats is approximately 6.3 times the equivalent human dose[17]. The rats in the treatment group were intraperitoneally injected with AI 0.4, 0.8, and 1.6 mL/kg for 10 weeks; the control group and DCI group received the same volume of normal saline (Figure 1).

Cell culture

Rat brain microvascular endothelial cells (RBMECs, BNCC337717) were purchased from Beijing Beina Chuanglian Biotechnology Research Institute. The cells were cultured in high-glucose Dulbecco's modified Eagle medium (DMEM) supplemented with 10% fetal bovine serum (FBS), 100 U/mL penicillin/streptomycin in an incubator with 5% CO_2 at 37°C.

Experimental methods

Morris Water Maze

The MWM (ZH0065; Anhui Zhenghua Biological Apparatus Facilities Co., Ltd., Huaibei, China), which consists of a large circular pool (diameter, 150 cm; height, 60 cm) and a platform (diameter, 12 cm; height, 20 cm), has become a popular tool for evaluating spatial learning and memory[18]. The pool was divided into four quadrants, with different marks on the left and right sides of each quadrant's wall serving as visual cues. The pool was filled with water to a depth of 2 cm above the platform and maintained the water temperature at 25°C ± 2°C. Rats were required to undergo a 4-day training experiment to enhance memory and a 1-day spatial exploration experiment to evaluate the degree of memory. To get accustomed to the environment, the rats were placed in water for 90 seconds the day before training. In each training session, the rats were slowly placed in the water facing the mark in the second quadrant, and the time taken to reach the platform was recorded. The upper limit was 90 seconds, and the time allowed to stand on the platform was 20 seconds. The time taken to find the platform is called the escape latency, and the time spent in the target quadrant indicates the degree of memory used after learning and training. On day 5, the space exploration experiment was conducted, the platform in the pool was removed, and the rats were slowly placed into the water from quadrant 2 facing the mark; escape latency, times across the platform, times in the target quadrant, and mean swimming speed were recorded within 90 seconds.

Hematoxylin–eosin (HE) staining and Nissl staining

The whole brain of the rat was collected, and the hippocampus of the left cerebral hemisphere was stripped and stored in cryopreserved tubes at –80°C; meanwhile, the right was taken into 4% paraformaldehyde for 48 hours and finally embedded in the paraffin through dehydration by gradient ethanol, obliteration by xylene, and debenzolization by paraffin. The brains were coronally cut into 5 μm sections that contained the complete hippocampus, then the sections were baked in the oven for 30 minutes at 60°C and stored at 4°C. After dewaxing with xylol, debenzolization with ethanol, and rehydration with distilled water, the nuclei were stained for 8 minutes with hematoxylin. The sections for 20 seconds with 1% hydrochloric acid alcohol, and the cytoplasm was stained for 1 minute with eosin. Brain sections were observed, and images of the CA1 and CA3 regions of the hippocampus

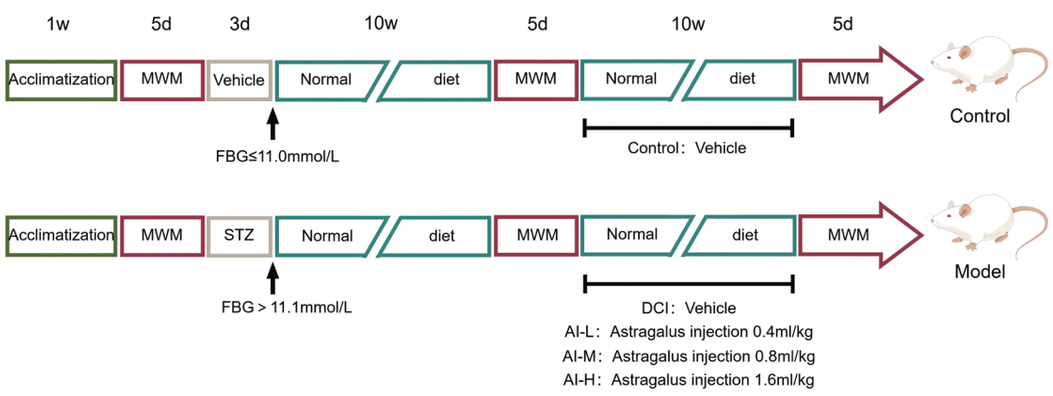


Figure 1. Specific modeling, grouping, and intervention process of the control and DCI rats. DCI: Cognitive Impairment of Diabetes; FBG: Fasting blood glucose; MWM: Morris Water Maze; STZ: Streptozotocin.

HM9_V6N2.indb 232 25-Jun-26 00:45:11

were captured using an optical microscope (Olympus, Tokyo, Japan). To better calculate the neuron numbers, the sections were stained with 0.1% toluidine blue for 3 minutes. High magnification (400×) was used to quantify the neuronal density as the average number of surviving hippocampal CA1 and CA3 pyramidal neurons.

Network pharmacology

The drug targets related to AI were collected from the Traditional Chinese Medicine System Pharmacology Database and Analysis Platform (Traditional Chinese Medicines Systems Pharmacology [TCMSP], http://tcmspw.com/tcmsp.php). Compounds with oral bioavailability ≥30% and drug-likeness ≥0.18 were selected. The literature has been consulted for additional major chemical components. The PubChem database (https://pubchem.ncbi.nlm.nih.gov) was searched for SMILES of obtained compounds, and the SMILES were entered into Swiss Target Prediction (http://www.swisstargetprediction.ch). As a result, we acquired the potential targets of the primary active chemical composition and selected the target with a predicted score greater than 0 as the drug target. DCI-related targets were retrieved from on-line Mendelian Inheritance in Man (OMIM, https://www.omim.org), GeneCards (https://genealacart.genecards.org), Pharmacogenetics and Pharmacogenomics Knowledge Base (PharmGkb, https://www.pharmgkb.org), and to obtain the Uniprot ID of each target gene, we removed all the targets after normalizing and importing them into Uniprot (https://www.uniprot.org/). Potential targets for the AI treatment of DCI were obtained by intersecting AI drug targets with DCI-related targets. These targets were imported into Cytoscape 3.8.0 to construct a drug-component-target-disease interaction network that visualized and integrated topological parameters. The identified potential proteins were imported to the String database (https://string-db.org/), and limited the species to "Homo sapiens." The minimum required interaction score was set to the highest confidence (0.900) to obtain corresponding relationships about protein interactions. Using the STRING database, all known and predicted protein functional associations were collected and integrated into the functional connections of the protein network, and Cytoscape 3.8.0 was used to construct the protein–protein interaction (PPI) network. Next, CytoNCA was used for optimization. Goplot in the R software was used to perform Gene Ontology (GO) enrichment and Kyoto Encyclopedia of Genes and Genomes (KEGG) pathway enrichment analyses for the key targets. Using $P < 0.05$ as the significant enrichment criterion.

Screening of optimal modeling agent and drug intervention concentrations using the CCK-8 assay

This study employed the Cell Counting Kit-8 (CCK-8) assay to conduct cellular modeling and drug concentration screening experiments. RBMECs were seeded in 96-well plates at a density of 5×10^3 cells/well and cultured for 24 hours at 37°C with 5% CO_2 until complete cell adhesion was achieved. Subsequently, the cells were treated with varying concentrations of the modeling agents and gradient concentrations of AI. After treatment, 10 µL of CCK-8 reagent was added to each well, followed by additional incubation for 2 to 4 hours. The absorbance of each well was measured at 450 nm by using a microplate reader.

Determination of biochemical indicator

Blood glucose levels were measured in rat tail vein blood samples using a glucometer (URIT, Guilin, China) after overnight fasting. Blood samples were collected *via* the femoral artery and centrifuged at 3,000 rpm for 15 minutes. The obtained serum was aliquoted into centrifuge tubes and stored at –80°C until analysis. The concentrations of MDA and SOD were determined in both serum and cellular samples, and catalase (CAT) and glutathione peroxidase (GSH-Px) levels were measured in serum samples.

ELISA assays

Levels of TNF-α, IL-1β in the serum and Nrf2, TNF-α, IL-1β, and IL-10 in the supernatant of the hippocampus were assayed by ELISA. The absorbance was measured at 450 nm using an ELISA multimode plate reader (PerkinElmer, Waltham, MA, USA).

Real-time polymerase chain reaction analysis

Total RNA was extracted from the homogenized 30 mg hippocampal tissue samples using TRIzol reagent kits and the Transcription First Strand cDNA Synthesis Kit (Tiangen Biotech, Beijing, China). Quantitative real-time polymerase chain reaction (RT-PCR) was initiated with 1 µL cDNA using SYBR Green PCR reagent kit (Tiangen Biotech) by 7500 fast Real-time System (ABI, Foster City, CA, USA). The primer sequences used for RT-PCR analysis are listed in Table 1. The program settings were as follows: pre-denaturation at 95°C for 10 minutes, denaturation at 95°C for 15 seconds, annealing at 60°C for 1 minute, 40 cycles. Relative mRNA values were normalized to the GAPDH gene control values and were calculated using the comparative cycle threshold method ($2^{-\triangle\triangle CT}$).

Immunohistochemistry

After pretreatment with 3% H_2O_2 for 10 min at room temperature, paraffin sections were immersed in citrate buffer (pH 6.0) and microwaved for 15 minutes. To block nonspecific sites, after three times washing with phosphate-buffered saline (PBS), the slides were incubated with 5% goat serum for 30 minutes at 37°C. Sections were incubated with mouse monoclonal antibody TLR-4 (1:100; Santa Cruz, Dallas, TX, USA) and TNF-α (1:100; Boster, Wuhan, China) overnight at 4°C. After washing, the sections were incubated with horseradish peroxidase (HRP) enzyme labeling second antibody IgG (goat anti-mouse IgG H&L [HRP], goat anti-rabbit IgG H&L [HRP]; Boster) at 37°C for 30 min. The cells were then washed thrice with PBS for 5 minutes. Subsequently, hippocampal sections were stained with diaminobenzidine (DAB) to visualize the pyramidal

HM9_V6N2.indb 233 25-Jun-26 00:45:11

Table 1

Primer sequences used in real-time RT-PCR

Gene	Primer sequences(5'–3')	PCR product size
TLR-4	Forward, 5'-TGGCATCATCTTCATTGTCC-3'	115 bp
	Reverse, 5'-CAGAGCATTGTCCTCCCACT-3'	
TNF-α	Forward, 5'-TCGTAGCAAACCACCAAGC-3';	148 bp
	Reverse, 5'-TGGAAGAGAACCTGGGAGTAGA-3'	
IL-1β	Forward, 5'-GCCAACAAGTGGTATTCTCCA-3'	118 bp
	Reverse, 5'-CCGTCTTTCATCACACAGGA-3'	
Nrf2	Forward, 5'- CTGCTGCCATTAGTCAGTCG-3'	101 bp
	Reverse, 5'- GCCTTCAGTGTGCTTCTGGT-3'	
GAPDH	Forward, 5'-GTTACCAGGGCTGCCTTCTC-3'	177 bp
	Reverse, 5'-GATGGTGATGGGTTTCCCGT-3'	

IL-1β: Interleukin-1β; Nrf2: Nuclear factor-erythroid-derived–related factor 2; TLR: Toll-like receptor; TNF-α: Tumor necrosis factor-α.

cells. The nuclei of the cells were counterstained with hematoxylin, and the sections were dehydrated with conventional gradient alcohol, observed, and photographed under a microscope.

Western blot analysis

The hippocampal tissues stored at −80°C and cells from the cell culture incubator were homogenized in ice-cold radioimmunoprecipitation assay (RIPA) lysis buffer (containing protease and phosphatase inhibitor cocktail; Beyotime Biotechnology, Shanghai, China). The protein concentration of the samples was determined using a bicinchoninic acid (BCA) kit (Beyotime Biotechnology). The samples were subjected to sodium dodecyl sulfate-polyacrylamide gel electrophoresis (SDS-PAGE) and transferred onto polyvinylidene difluoride membranes using an electrophoretic transfer system. The membranes were blocked with tris-buffered saline mixed with tween-20 (TBST) containing 5% skim milk for 60 minutes. After overnight incubation at 4°C, various antibodies were used to probe the membranes, including p-IκB-α, IκB-α, NF-κBp65, and Nrf2 (all diluted 1:500; ZSGB-BIO, Beijing, China). Incubation with secondary antibodies conjugated with HRP was performed after washing the membranes (diluted 1:20,000; ZSGB-BIO) for 1 hour at 37°C. Binding was detected using an enhanced chemiluminescence (ECL) detection reagent.

Statistical analysis

The data are expressed as the mean ± standard error. SPSS statistical software (SPSS 19.0 version; SPSS Inc., Chicago, IL, USA) was used for the statistical analysis, using one-way analysis of variance (ANOVA) followed by the Dunnett's test for individual comparisons between groups. Statistical significance was set at $P < 0.05$.

Results

AI improves cognitive impairment and ameliorates hyperglycemia in DCI rats

To verify whether AI can improve cognitive function in rats with DCI, we performed an MWM experiment. By analyzing the trajectories in the water maze, it was found that the rats in the control group could find the hidden platform in the water rapidly, whereas the movement paths of the rats in the DCI group were extended and messy, and they could not find the platform within a set time. The AI-L, AI-M, and AI-H groups were able to find the platform in the water more smoothly (Figure 2A). In the acquisition phase, it was found by recording and analyzing the escape latency of each group of rats that with the increase in training days, the escape latency of all five groups of rats decreased, and the escape latency of the DCI group significantly increased in comparison to the control group. After 10 weeks of drug treatment, the escape latencies of the AI-L, AI-M, and AI-H groups were significantly reduced (Figure 2B). In the space exploration test, the mean swimming speed, times across the platforms, and times in the target quadrant of rats in the DCI group were significantly reduced compared to the control group. After AI treatment, the mean swimming speed, times across the platforms, and times in the target quadrant of rats in the AI-L, AI-M, and AI-H groups were significantly increased (Figure 2C–E).

Because hyperglycemia is an important clinical symptom in patients with DCI, we measured FBG levels in each group at three time points: at the start of the experiment, before AI treatment, and after AI treatment. According to the results, at the start of the experiment, the FBG of each group of rats was at normal levels (FBG ≤11.0 mmol/L)[19]; before AI treatment, in comparison with the control group, the FBG of the DCI, AI-L, AI-M, and AI-H groups significantly increased; after AI treatment, the FBG of rats in the AI-L, AI-M, and AI-H groups was significantly reduced compared with the DCI group (Figure 2F).

AI attenuates neuronal damage in DCI rats

Owing to the frequent occurrence of hippocampal damage in patients with DCI[20], we observed morphological changes in the hippocampal tissues of each group of rats using HE and Nissl staining. According to the HE staining results, the CA1 and CA3 regions of the control rats' hippocampus contained two to three layers of small

HM9_V6N2.indb 234 25-Jun-26 00:45:11

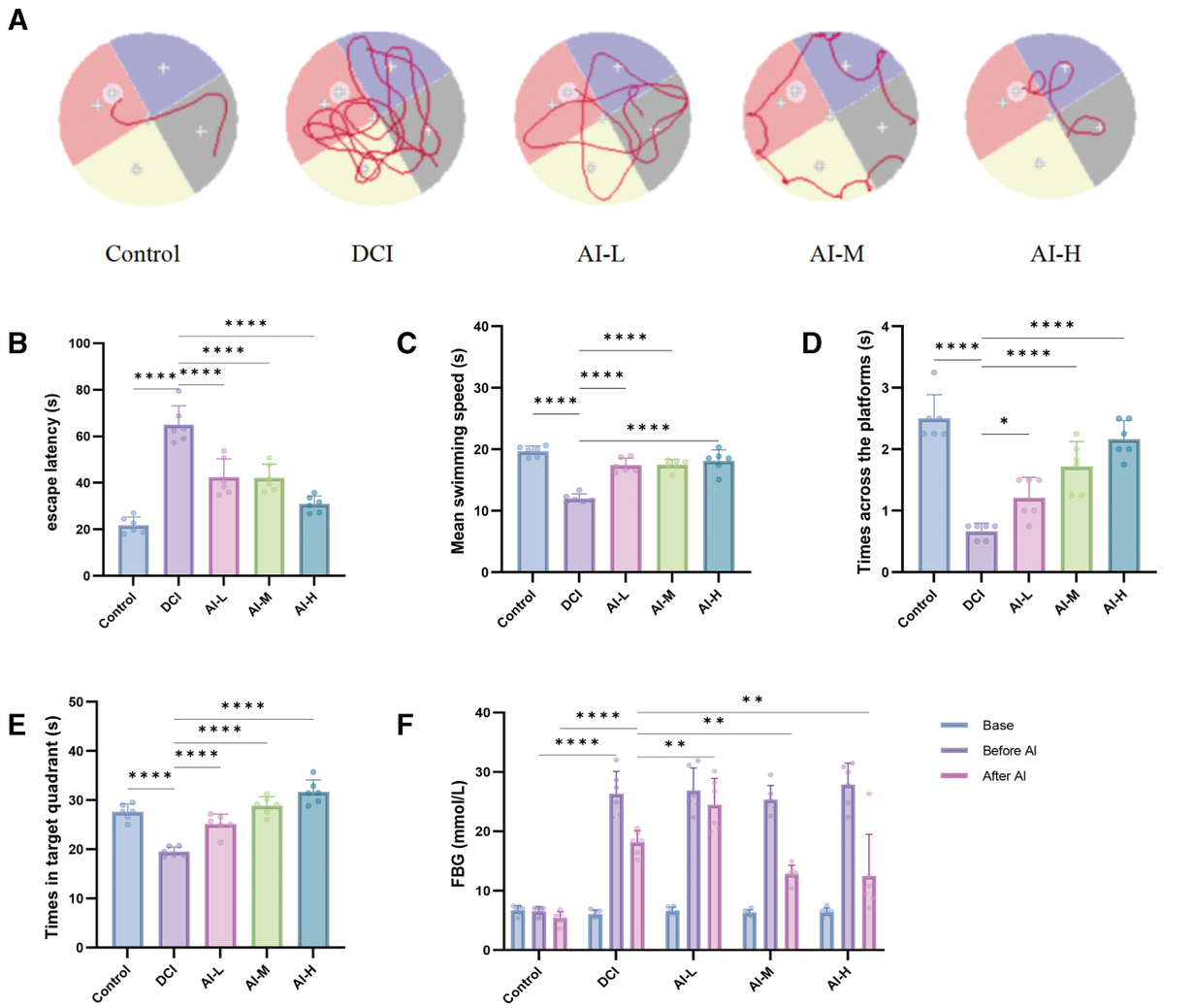


Figure 2. AI improved cognitive function and lowered blood sugar in DCI rats. (A) The swimming traces of each group of rats during the space exploring test. (B) The escape latency in each water maze test group during the acquisition phase. (C–E) The mean swimming speed, times across the platforms, and times in the target quadrant in the space exploring test. (F) Levels of FBG in rats within each experimental group. Data were expressed as mean ± standard error. *$P < 0.05$, **$P < 0.01$, ****$P < 0.0001$ compared to the DCI group. AI: Astragalus injection; DCI: Cognitive Impairment of Diabetes; FBG: Fasting blood glucose.

pyramidal cells, with full and tightly arranged nuclei, deep-stained nucleoli, clear boundaries, and light-stained cytoplasm. The hippocampal CA1 and CA3 regions of the DCI group were observed to have abnormal structures and morphologies compared to those of the control group. The arrangement of pyramidal cells gradually became loose and irregular in shape, and the boundary between the nucleus and cytoplasm became unclear. Some neurons were gradually lost, accompanied by eosinophilic cytoplasm and dense triangular nuclei. After 10 weeks of AI treatment, the neurons in the hippocampal CA1 and CA3 regions of rats in the AI-L, AI-M, and AI-H groups were arranged in a more regular and orderly manner than those in the DCI group, with clear cell structures and no significant neuronal damage (Figure 3A).

According to the Nissl staining results, the CA1 and CA3 hippocampal neurons in the control group rats showed clear and intact structures, with Nissl bodies distributed evenly around the nucleus and clearly visible neuronal axons. By analyzing the images with ImageJ, we found that a considerable number of neurons in the DCI group were damaged, characterized by the loss of cell integrity, cytoplasmic atrophy, Nissl body condensation, and blurred nuclei, and the number of healthy neurons declined significantly. In the AI-L, AI-M, and AI-H groups, the hippocampal CA1 and CA3 regions were tightly arranged, which was significantly reversed after 10 weeks of AI treatment. The cytoplasmic content of Nissl bodies increased, indicating a significant reduction in the symptoms of neuronal damage (Figure 3B–D).

Network pharmacology results

Active components in Astragalus membranaceus and target prediction

By retrieving the TCMSP and meeting the screening criteria (oral bioavailability ≥30% and drug-Likeness ≥0.18), a total of 20 active components of Astragalus

HM9_V6N2.indb 235 25-Jun-26 00:45:12

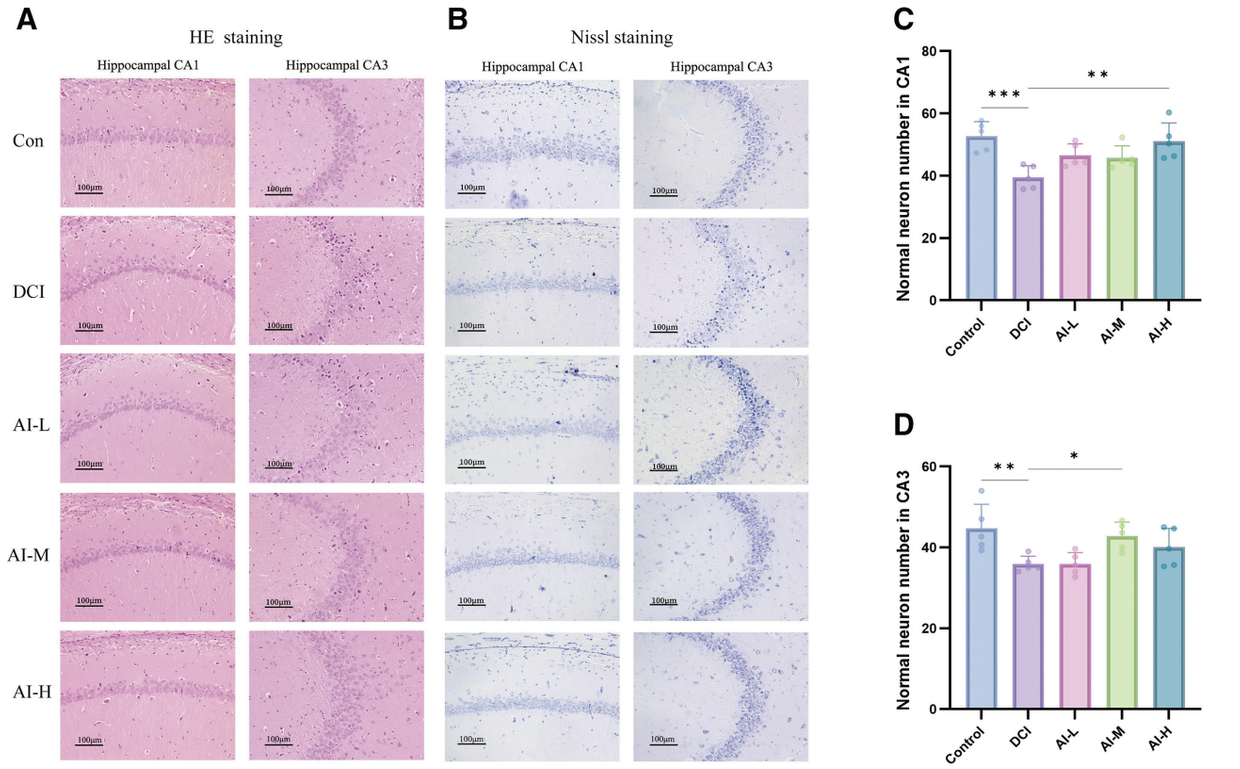


Figure 3. AI reduced neuronal damage in DCI rats. (A) HE staining of hippocampal CA1 and CA3 regions (200×, scale bar = 100 μm). (B) Nissl staining of hippocampal CA1 and CA3 regions (400×, scale bar = 100 μm). (C) Number of neurons in the hippocampal CA1 region. (D) Number of neurons in the hippocampal CA3 region. Data were expressed as mean ± standard error. *$P < 0.05$, **$P < 0.01$, ***$P < 0.001$ compared to DCI group. AI: Astragalus injection; DCI: Cognitive Impairment of Diabetes; HE: Hematoxylin-eosin.

membranaceus were selected, five components including Astragaloside I, Astragaloside II, Astragaloside III, Astragaloside IV, and Astragalus membranaceus polysaccharides were supplemented through literature. Finally, 25 potentially active components were obtained[21]. A total of 537 drug targets of the effective components were retrieved from the Swiss Target Prediction Database. The full name of the gene was converted to a gene symbol using the UniProt database, duplicate values were eliminated, and 251 targets remained. The active components of Astragalus membranaceus are listed in Table 2.

Potential targets prediction of DCI

By searching the GeneCards, OMIM, and PharmGkb databases, 7,967, 179, and 103 DCI targets were obtained, respectively. We merged the targets from the three databases, removed duplicates, and obtained 8,036 DCI-related targets. By considering the intersection of Astragalus membranaceus drug targets and DCI-related targets, 220 intersection targets were obtained, which were potential targets for AI in the treatment of DCI (Figure 4A).

Construction of drug-component-target-disease interaction network

Twenty-five potentially active components and 220 drug-disease common targets in Astragalus membranaceus were input into Cytoscape 3.8.0; the isolated components that did not intersect with the target were deleted, and the drug-component-target-disease interaction network was drawn. A network analyzer was used to perform topology analysis on the network diagram, where the degree value represented the number of associations between the active components and the target. The higher the degree value, the more important the component. The results illustrated that Quercetin, kaempferol, 2-(Chloromethyl)-4-(4-nitrophenyl)-1,3-thiazole, formononetin, isorhamnetin, and Astragaloside I–IV exhibited high levels of activity, suggesting that these components may be responsible for the pharmacological effects of AI (Figure 4B).

PPI network construction and key targets

Using the STRING database, a PPI network with 179 nodes and 1,138 edges was constructed to identify the core proteins for AI intervention in DCI (Figure 4C, a). Betweenness centrality (BC), Closeness Centrality, Degree Centrality (DC), Eigenvector Centrality (EC), Local Average Connectivity-based method (LAC), and Network Centrality (NC) of each target protein were calculated using CytoNCA. According to BC ≥90.73 (average), CC ≥0.06 (average), DC ≥8.00 (average), EC ≥0.02 (average), LC ≥4.00 (average), NC ≥4.57 (average), 49 target proteins were screened, and subnetworks were created (Figure 4C, b) with 49 nodes and 456 edges. Again, CytoNCA was used to calculate the BC, Closeness Centrality, DC, EC, LAC, and NC of the target

HM9_V6N2.indb 236 25-Jun-26 00:45:12

Table 2

Active components of Astragalus membranaceus

MOL ID	Component name	Oral bioavailability %	Drug-likeness
MOL000211	Mairin	55.38	0.78
MOL000239	Jaranol	50.83	0.29
MOL000296	Hederagenin	36.91	0.75
MOL000033	(3S,8S,9S,10R,13R,14S,17R)-10,13-dimethyl-17-[(2R,5S)-5-propan-2-yloctan-2-yl]-2,3,4,7,8,9,11,12,14,15,16,17-dodecahydro-1H-cyclopenta[a]phenanthren-3-ol	36.23	0.78
MOL000354	Isorhamnetin	49.6	0.31
MOL000371	3,9-Di-*O*-methylnissolin	53.74	0.48
MOL000374	5'-Hydroxyiso-muronulatol-2',5'-di-O-glucoside	41.72	0.69
MOL000378	7-*O*-Methylisomucronulatol	74.69	0.3
MOL000379	9,10-Dimethoxypterocarpan-3-*O*-β-*D*-glucoside	36.74	0.92
MOL000380	(6aR,11aR)-9,10-Dimethoxy-6a,11a-dihydro-6H-benzofurano[3,2-c]chromen-3-ol	64.26	0.42
MOL000387	Bifendate	31.1	0.67
MOL000392	Formononetin	69.67	0.21
MOL000398	Isoflavanone	109.99	0.3
MOL000417	Calycosin	47.75	0.24
MOL000422	Kaempferol	41.88	0.24
MOL000433	Ferulic acid	68.96	0.71
MOL000438	(3R)-3-(2-Hydroxy-3,4-dimethoxyphenyl)chroman-7-ol	67.67	0.26
MOL000439	Isomucronulatol-7,2'-di-*O*-glucosiole	49.28	0.62
MOL000442	1,7-Dihydroxy-3,9-dimethoxy pterocarpene	39.05	0.48
MOL000098	Quercetin	46.43	0.28
MOL000401	Astragaloside I	46.79	0.11
MOL000403	Astragaloside II	46.06	0.13
MOL000405	Astragaloside III	31.83	0.10
MOL000407	Astragaloside IV	46.06	0.18
–	Astragalus polysaccharides	–	–

proteins in the subnetwork. According to BC ≥12.67 (average), CC ≥0.48 (average), DC ≥16.00 (average), ≥EC 0.11 (average), LAC ≥8.00 (average), NC ≥9.23 (average), 13 target proteins were screened, and there were 13 nodes and 92 edges in the diagram (Figure 4C, c). These 13 proteins are key target proteins of AI in the treatment of DCI.

GO enrichment and KEGG enrichment

Subsequently, based on the potential targets of AI, GO, and KEGG functional enrichment analyses were conducted to explore the potential signaling pathways or biological processes (BP) that may be regulated by AI. According to GO analysis, 220 genes were enriched in 2,998 GO entries ($P < 0.05$), including 2,656 BP, 113 cellular components, and 229 molecular functions (MF), and the top 10 entries of BP, cellular component, and MF are shown in Figure 4D. BP analysis indicated that potential targets were predominantly concentrated on the response to xenobiotic stimulus, response to lipopolysaccharide, response to nutrient levels, response to molecules of bacterial origin, and wound healing. Cellular component analysis indicated that potential targets were predominantly concentrated on membrane rafts, membrane microdomains, integral components of the presynaptic membrane, and potential targets were identified as G protein–coupled amine receptors, neurotransmitter receptors, nuclear receptors, etc, based on MF analysis. KEGG functional enrichment analysis indicated 179 pathways, among which pathways related to DCI were primarily associated with pathways in cancer, calcium signaling, p53 signaling, vascular endothelial growth factor (VEGF) signaling, and Toll-like receptor (TLR) signaling pathway. Based on the *P* value, the top 20 signaling pathways were chosen for visual display (Figure 4E). The color represents enrichment significance; if the color is darker, the target protein is more significant in this pathway, and the *P* value is smaller.

Animal experiment results

AI alleviates oxidative stress in DCI rats

As shown in Figure 5, MDA levels increased in the DCI group, whereas SOD, CAT, and GSH-Px levels were comparatively lower than those in the control group. The AI groups exhibited a notable reduction in MDA

HM9_V6N2.indb 237 25-Jun-26 00:45:13

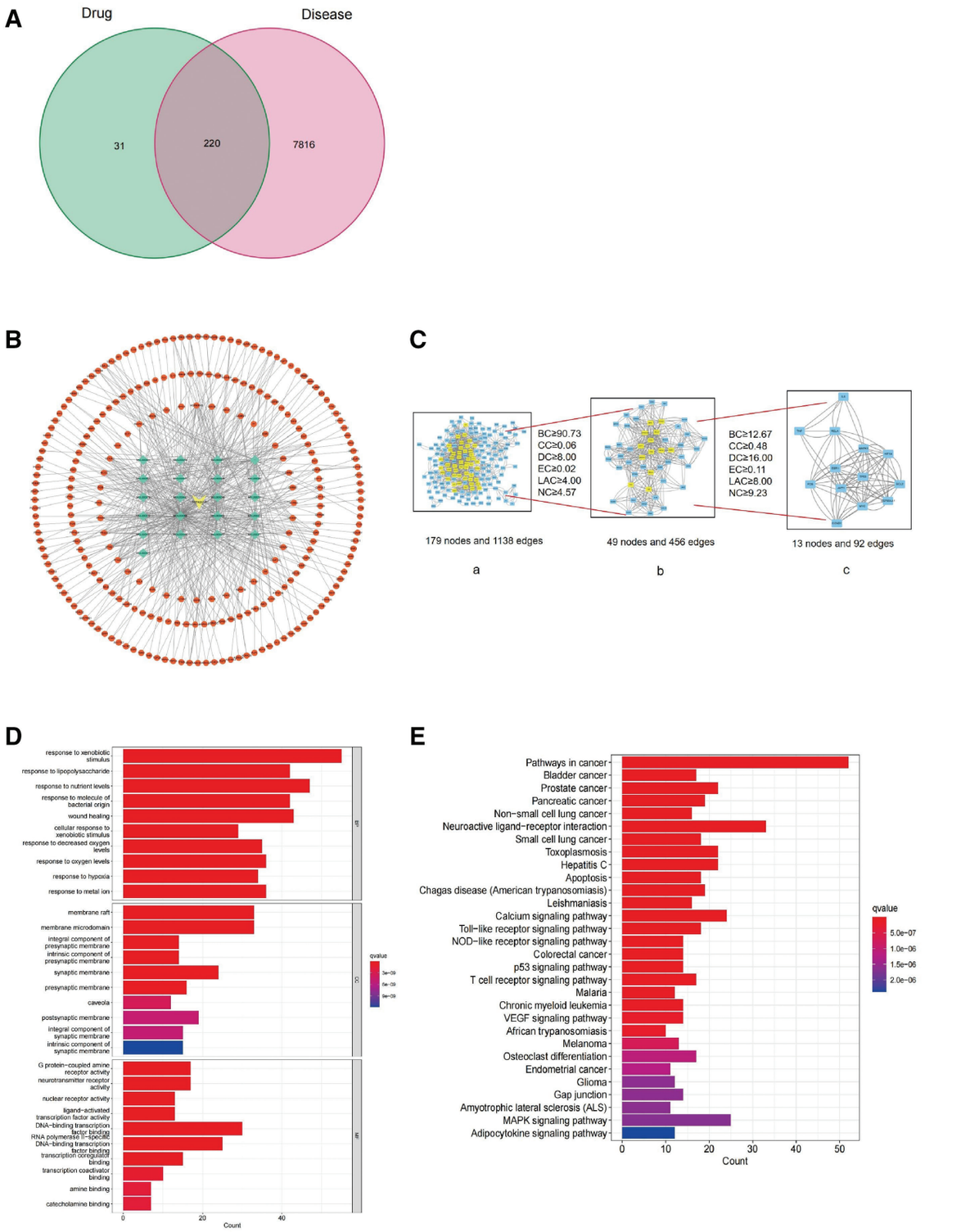


Figure 4. Complete network pharmacology flowchart of the mechanism of AI treatment for DCI. This includes (A) potential target identification, (B) construction of the drug-component-target-disease interaction network, (C) PPI network and cluster analysis of the disease targets, (D) GO, and (E) KEGG functional analysis. AI: Astragalus injection; DCI: Cognitive Impairment of Diabetes; GO: Gene Ontology; PPI: protein–protein interaction; KEGG: Kyoto Encyclopedia of Genes and Genomes.

levels following the AI intervention, in contrast to the DCI group. However, a dose-dependent increase in SOD, CAT, and GSH-Px levels was observed. Based on these results, it can be seen that AI has the effect of reducing DCI rats' oxidative stress.

AI exerts antioxidative stress by activating the Keap1/Nrf2 pathway

DCI has been demonstrated to be significantly influenced by oxidative stress. Nrf2 is an important transcription factor regulating antioxidative stress. It has been found

HM9_V6N2.indb 238 25-Jun-26 00:45:13

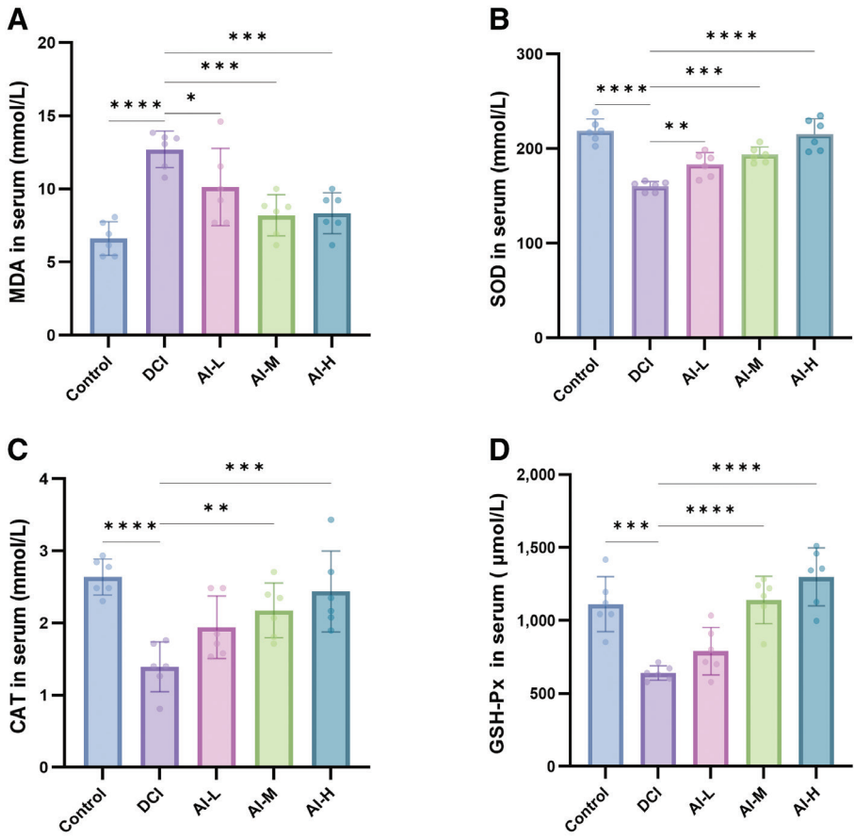


Figure 5. AI alleviated oxidative stress in DCI rats. The levels of serum (A) MDA, (B) Total SOD (T-SOD), (C) CAT, and (D) GSH-Px in each group of rats. Data were expressed as mean ± standard error. *$P < 0.05$, **$P < 0.01$, ***$P < 0.001$, ****$P < 0.0001$ compared to the DCI group. AI: Astragalus injection; CAT: Catalase; DCI: Cognitive Impairment of Diabetes; GSH-Px: Glutathione peroxidase; MDA: Malondialdehyde; SOD: Superoxide dismutase.

that the improvement of cognitive effect and neuronal function in DCI rats after AI treatment may be due to the increased activation of Nrf2 and its target genes. We evaluated the Nrf2 and Keap1 mRNA levels in the hippocampus using RT-PCR. The DCI group experienced a notable decrease in the mRNA expression of these factors (Figure 6A and B), compared with the DCI group, this downward trend in the AI groups was alleviated in a dose-dependent manner. ELISA was used to study the effect of AI on Nrf2 protein expression in the hippocampi of DCI rats. The DCI group had significantly decreased Nrf2 protein levels, whereas the AI group had dose-dependently increased Nrf2 levels (Figure 6C). Overall, we believe that the effect of AI on DCI may be attributable to the activation of Nrf2 and its upstream genes.

By detecting the expression of Nrf2 protein in the total hippocampal, nuclear, and cytoplasmic extracts of each group, western blotting revealed that AI treatment led to a significant increase in nuclear Nrf2 expression compared to that in the DCI group, suggesting enhanced nuclear translocation of Nrf2 in rat neurons (Figure 6D–G). These findings indicate that AI can activate the Keap1/Nrf2 signaling pathway.

AI mitigates neuroinflammation in DCI rats

STZ-induced DCI rats had significantly higher serum levels of TNF-α and IL-1β in contrast to the control group. However, after 10 weeks of AI treatment, serum TNF-α and IL-1β levels were significantly lower than in the DCI group (Figure 7A). The DCI group exhibited notable elevations in TNF-α and IL-1β protein and mRNA expression, while IL-10 decreased when compared to the control group. In AI groups, both TNF-α and IL-1β proteins and mRNA levels declined while IL-10 levels increased compared to the DCI group (Figure 7B and C).

AI exerts an anti-neuroinflammation effect by inhibiting the TLR-4/NF-κB pathway

Based on immunohistochemical staining, the CA1 and CA3 of the hippocampus in the DCI group indicated a significant increase in levels of TLR-4 and TNF-α than in the control group. After 10 weeks of AI treatment, TLR-4 and TNF-α expression in the hippocampus were significantly declined (Figure 8A–D). Additionally, western blots were also performed to investigate the effects of AI on the NF-κB signal pathway. According to the results, the DCI group had significantly higher levels of IκB-α phosphorylation and NF-κBp65 protein expression than the control group, and AI therapy could decrease IκB-α phosphorylation. Although the inhibitory effect of AI on the expression of NF-κBp65 protein in DCI rats showed an increasing trend with the increase of dose, there was no statistical significance. The DCI group exhibited a notably elevated ratio of p-IκB-α/IκB-α in comparison

HM9_V6N2.indb 239 25-Jun-26 00:45:14

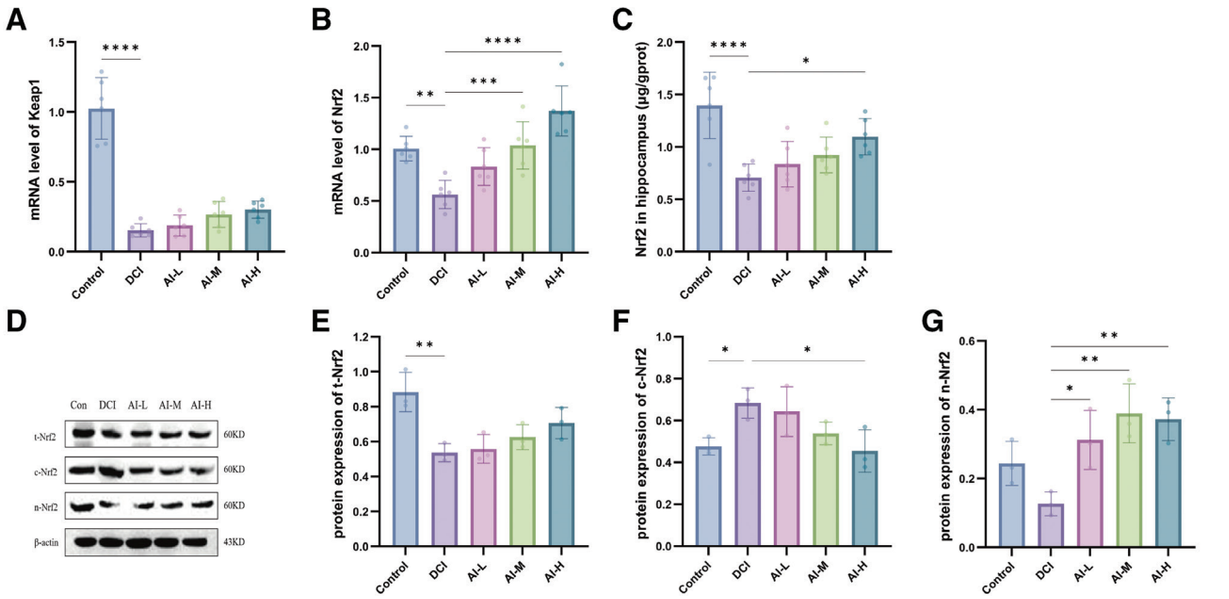


Figure 6. AI activates the Keap1/Nrf2 pathway. (A–B) Nrf2 and Keap1 mRNA levels in the hippocampus of rats in each group. (C) Nrf2 protein levels in the hippocampus. (D) Representative bands from Western blot data. (E) Quantitative analysis of t-Nrf2 western blot bands. (F) Quantitative analysis of c-Nrf2 western blot bands. (G) Quantitative analysis of n-Nrf2 western blot bands. Data were expressed as mean ± standard error. *$P < 0.05$, **$P < 0.01$, ***$P < 0.001$, ****$P < 0.0001$compared to the DCI group. AI: Astragalus injection; DCI: Cognitive Impairment of Diabetes; Keap1: Kelch-like ECH-associated protein; Nrf2: Nuclear factor-erythroid-derived related factor 2.

to the control group, and 10 weeks after administration in AI groups, a dose-dependent decline in p-IκB-α/IκB-α ratio was observed in AI groups, particularly in AI-H. The NF-κBp65 level in the DCI group showed a significant increase when compared to the control group, while AI treatment reduced NF-κBp65 levels in dose-dependent ways (Figure 8E–G). The findings indicate that AI can suppress the neuroinflammation pathway mediated by TLR-4/NF-κB.

Cell experiment results

Screening of optimal concentrations for hydrogen peroxide and lipopolysaccharide

To determine the optimal intervention concentrations of hydrogen peroxide (H_2O_2) and lipopolysaccharide (LPS) for establishing oxidative stress and inflammatory cell models, cell viability was assessed using the CCK-8 assay after treatment with different concentrations of the modeling agents. Oxidative Stress Model: H_2O_2 was diluted in cell culture medium to various concentrations and applied to cells for 6 hours. The CCK-8 assay revealed that 400 μM H_2O_2 significantly reduced cell viability compared to the control group, with the inhibition rate approached 50%. Subsequent measurements using MDA and SOD assay kits confirmed that the model group exhibited significantly altered levels of MDA and SOD compared to the control group, indicating successful establishment of the oxidative stress model.

LPS was dissolved and diluted in the cell culture medium and used to incubate the cells for 24 hours. The CCK-8 assay showed that 400 μg/mL LPS significantly decreased cell viability compared to the control group, with the inhibition rate approached 50%. Further analysis using ELISA kits demonstrated that the model group had significantly elevated levels of IL-1β and TNF-α compared to the control group, confirming the successful replication of the inflammatory cell model (Figure 9A–F).

Screening of optimal intervention concentrations for AI

To determine the optimal protective concentration of AI against oxidative stress- and inflammation-induced cellular damage, cell viability was assessed using the CCK-8 assay following treatment with varying drug concentrations.

The results demonstrated that 400 μg/mL AI significantly enhanced cell viability compared to the untreated oxidative stress and inflammation group (control), indicating its efficacy in alleviating cellular damage. Lower concentrations showed no significant protective effect. Based on these findings, 400 μg/mL AI was selected as the optimal intervention concentration for subsequent experiments (Figure 10A and B).

AI mitigates oxidative stress and inflammation in RBMECs

Western blot analysis of Keap1 and Nrf2 protein expression in RBMECs revealed that, compared to the DCI group, the AI-treated group exhibited significantly increased expression of both proteins, which is consistent with the animal experimental results. These findings suggest that AI exerts antioxidant effects by activating the Keap1/Nrf2 signaling pathway.

Furthermore, western blot analysis of the p-IκB-α/NF-κB signaling pathway in RBMECs demonstrated that, compared to the control group, the DCI group

HM9_V6N2.indb 240 25-Jun-26 00:45:15

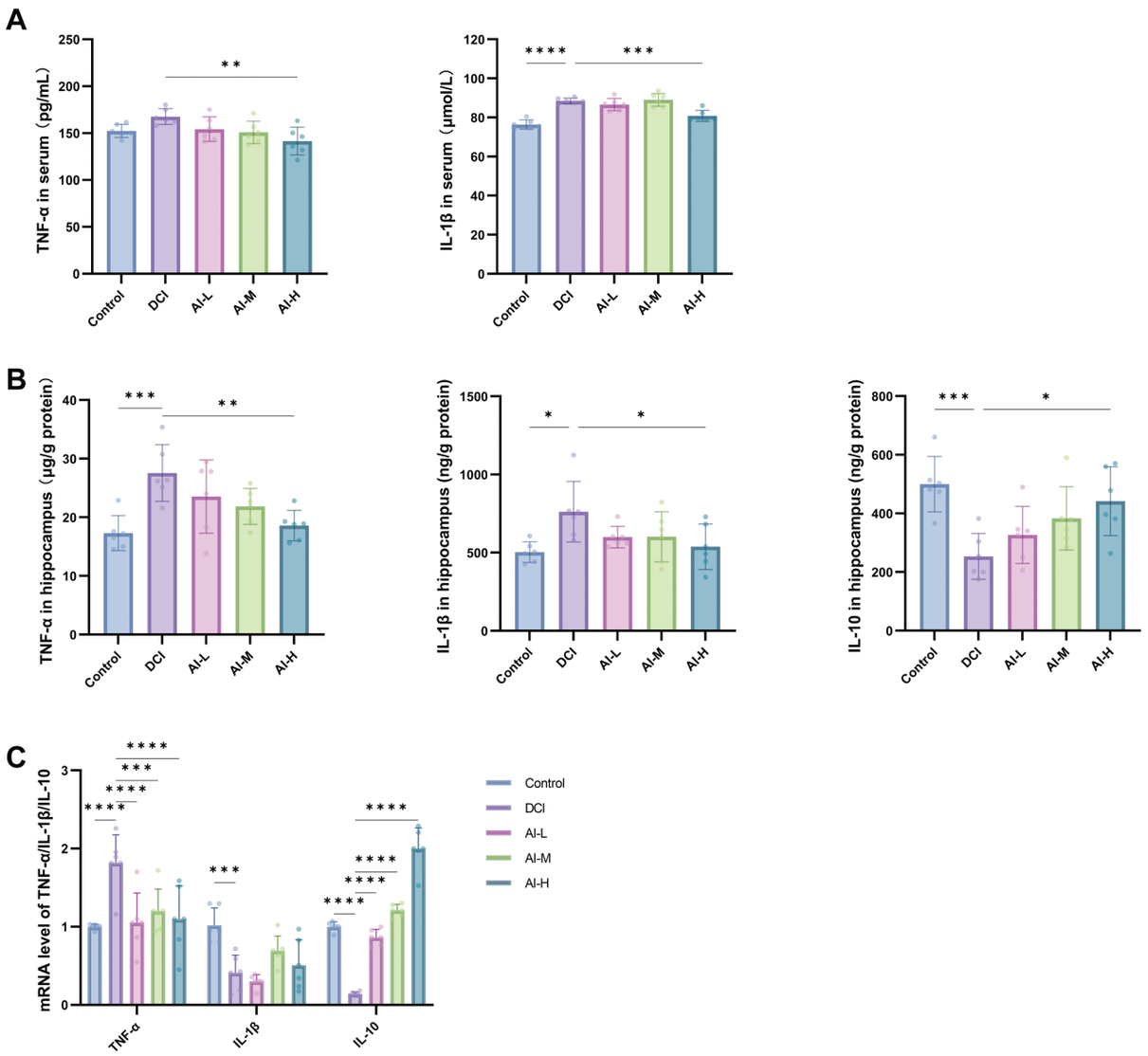


Figure 7. AI reduced neuroinflammation in DCI rats. AI's impact on (A) TNF-α and IL-1β serum levels of rats in each group, (B–C) TNF-α, IL-1β, IL-10 protein and mRNA levels in the hippocampus. Data were expressed as mean ± standard error. **P* < 0.05, ***P* < 0.01, ****P* < 0.001, *****P* < 0.0001compared to the DCI group. AI: Astragalus injection; DCI: Cognitive Impairment of Diabetes; IL: Interleukin; TNF-α: Tumor necrosis factor-α.

showed significantly elevated levels of p-IκB-α and NF-κB p65. However, AI treatment reduced IκB-α phosphorylation and NF-κB p65 expression, aligning with the *in vivo* observations. These results indicate that AI alleviates NF-κB–mediated inflammatory responses (Figure 11A–F).

Discussion

T1DM is a chronic autoimmune disease that affects many organs and is characterized by a lack of total insulin necessary for glucose metabolism, which can harm the brain. The hippocampus, situated deep in the medial temporal lobe of the brain, is responsible for consolidating episodic memory and context-sensitive spatial learning, along with regulating emotional behaviors[22]. Studies have demonstrated a significant reduction in CA1 and CA3 neurons within the hippocampus of diabetic rats, a phenomenon closely associated with DCI[23–24]. Despite this correlation, the specific pathogenesis of DCI remains largely unknown and there is no effective way to prevent or delay it. Therefore, the identification of effective drugs for the treatment of DCI is of great importance.

For millennia, evidence has suggested that Astragalus membranaceus can prevent and treat diabetes and its associated complications. Clinical practice indicates that Astragalus membranaceus exhibits promising efficacy in ameliorating memory impairment in patients with diabetes and may protect nerve cells through antioxidative, anti-infective, and anti-apoptotic functions. These findings suggest that Astragalus membranaceus could improve the cognitive function in individuals with diabetes to a certain degree[25–26]. However, further research is required to fully understand the specific mechanism. In light of this, our study conducted an experimental validation by utilizing AI as an intervention drug to

HM9_V6N2.indb 241 25-Jun-26 00:45:16

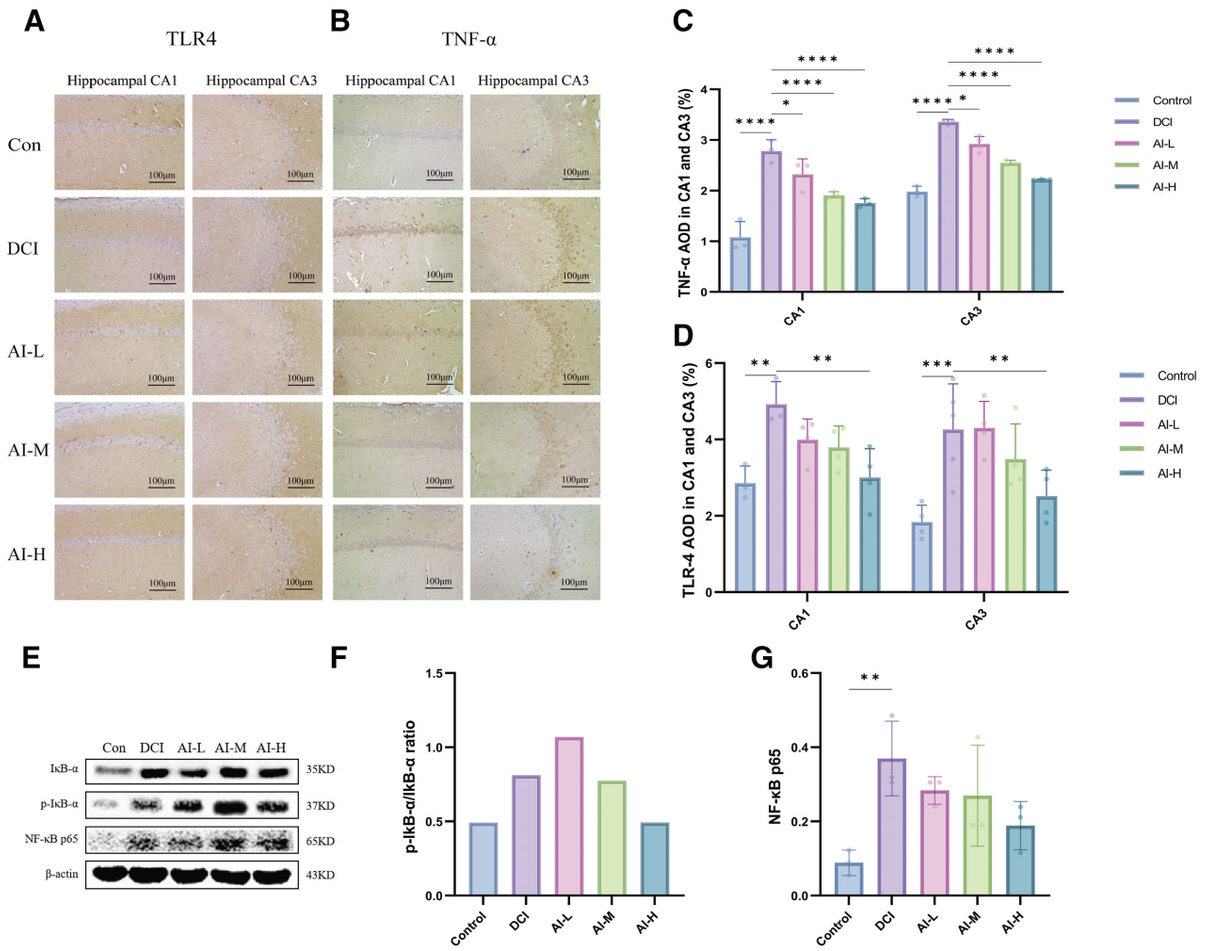


Figure 8. AI inhibited the TLR-4/NF-κB pathway. (A, C) Changes of TLR-4, TNF-α in the CA1 region of hippocampus and (B, D) changes of TLR-4, TNF-α in the CA3 region of hippocampus CA3 of rats in each group (200×, scale bar = 100 μm). AI's impact on the expression of (E, F) p-IκB-α, IκB-α, and (E, G) NF-κBp65 in the hippocampus. Data were expressed as mean ± standard error. *P < 0.05, **P < 0.01, ***P < 0.001, ****P < 0.0001 compared to the DCI group. AI: Astragalus injection; DCI: Cognitive Impairment of Diabetes; NF-κB: Nuclear factor-kappa B; TLR: Toll-like receptor; TNF-α: Tumor necrosis factor-α.

explore its effect on STZ-induced DCI in rats and its specific mechanism. The results indicated that AI improved blood glucose levels and cognitive ability of learning and memory in DCI rats in a dose-dependent manner. However, in the DCI group, FBG levels decreased after injection of normal saline, which may be related to other hypoglycemic hormones or substances in the body, such as leptin, insulin-like growth factor 1 (IGF-1), intestinal hypoglycemic hormone, intestinal microflora, and exogenous fibroblast growth factor 1 (FGF-1), and so forth[27–28]. The FBG levels were not significantly lower in the AI-L group than in the DCI group. This may be due to the drug concentrations. Subsequently, network pharmacology was used to screen potential targets of AI to alleviate DCI. Twenty-five kinds of potentially active components of Astragalus membranaceus were screened using the TCMSP database and literature. The primary active ingredients were quercetin, kaempferol, 2-(chloromethyl)-4-(4-nitrophenyl)-1-methyl-3-thiazole, formononetin, isorhamnetin, and Astragaloside I–IV and so forth. The core targets of Astragalus membranaceus related to DCI were screened by the PPI network, and the core signaling pathway of Astragalus membranaceus against DCI was screened by GO and KEGG enrichment analysis. The results showed that antioxidative and anti-neuroinflammation may be the dual mechanisms of AI in improving DCI.

Based on the network pharmacology results, we conducted an experimental verification. Oxidative stress is a primary factor contributing to the occurrence and development of DCI. Studies have shown that diabetics have heightened levels of oxidative stress and compromised antioxidant capacity, which is mainly characterized by an increase in the levels of reactive oxygen species (ROS) and MDA, and the inhibition of the activities of antioxidants SOD, CAT, and GSH-Px, resulting in damage to neurons and decreased cognitive function in patients with diabetes[29–30]. BMECs are the most critical structural components of the blood-brain barrier. Prolonged exposure to a hyperglycemic environment can disrupt the blood-brain barrier (BBB) integrity, leading to increased permeability. These pathological changes trigger neuroinflammation and oxidative stress, ultimately resulting in DCI[31]. In our study, AI was found to lower MDA levels and elevate SOD, CAT, and GSH-Px levels in DCI rats, confirming that AI could effectively alleviate oxidative

HM9_V6N2.indb 242 25-Jun-26 00:45:16

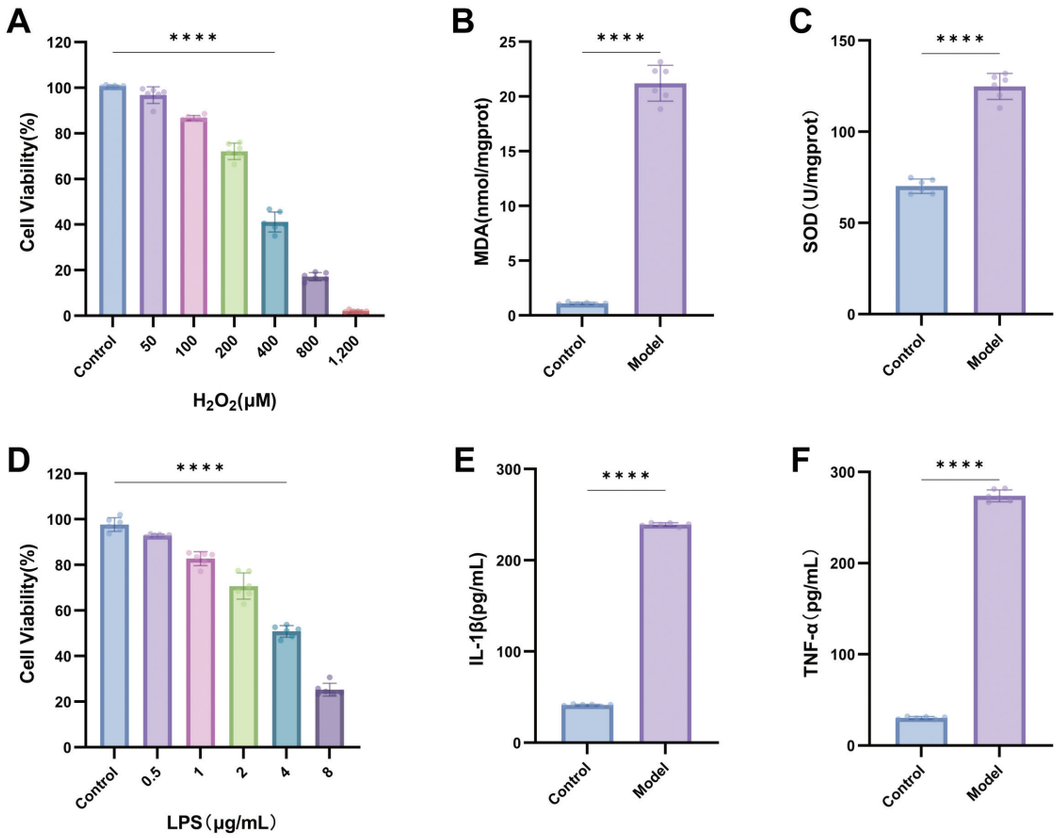


Figure 9. Screening of optimal concentrations for H_2O_2 and LPS. (A) Screening of H_2O_2 concentrations, (B) concentration of MDA in cells, (C) concentration of SOD in cells, (D) LPS concentration screening, (E) content of IL-1β in cells, (F) content of TNF-α in cells, data were expressed as mean ± standard error. ***$P < 0.001$ compared to the DCI group. H_2O_2: Hydrogen peroxide; IL-1β: Interleukin-1β; LPS: Lipopolysaccharide; MDA: Malondialdehyde; SOD: Superoxide dismutase; TNF-α: Tumor necrosis factor-α.

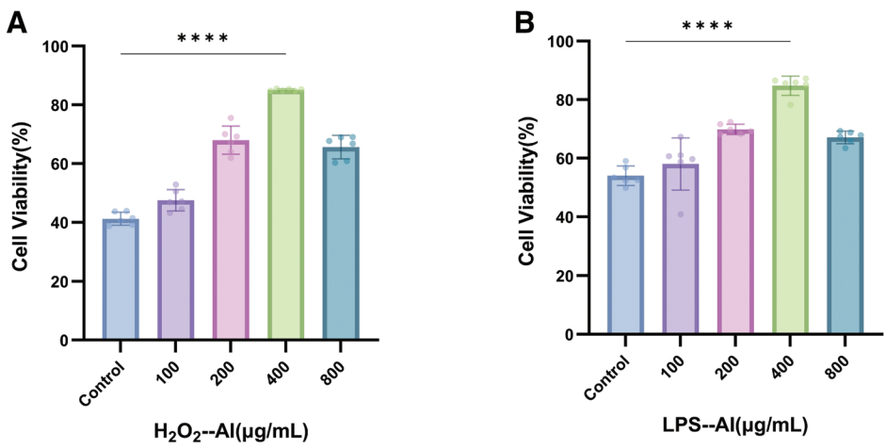


Figure 10. Optimization of AI concentration. (A) Optimization of AI concentration for oxidative stress models, (B) optimization of AI concentration for inflammatory models, data were expressed as mean ± standard error. ****$P < 0.0001$ compared to the DCI group. AI: Astragalus injection; DCI: Cognitive Impairment of Diabetes; H_2O_2: Hydrogen peroxide; LPS: Lipopolysaccharide.

damage induced by T1DM. In addition, many studies have shown that the neuritis cascade caused by the accumulation of pro-inflammatory cytokines TNF-α and IL-1β plays a vital role in DCI and may be the pathological basis for aggravating neurodegenerative diseases[32–33]. Compared to the DCI group, the AI groups significantly decreased and downregulated the levels and expression of TNF-α and IL-1β in the peripheral blood and hippocampus of rats, while IL-10 with an anti-inflammatory effect showed the opposite result. These results confirm that AI reduces the level of inflammation in DCI rats, especially neuroinflammation, thus treating DCI and relieving related symptoms. The *in vitro* experiments in this study revealed that AI exerts dual neuroprotective effects by simultaneously upregulating the expression of Keap1 and Nrf2 proteins to combat oxidative stress while suppressing the expression of p-IκB-α and NF-κB p65 proteins to mitigate inflammatory responses. These findings suggest

HM9_V6N2.indb 243 25-Jun-26 00:45:17

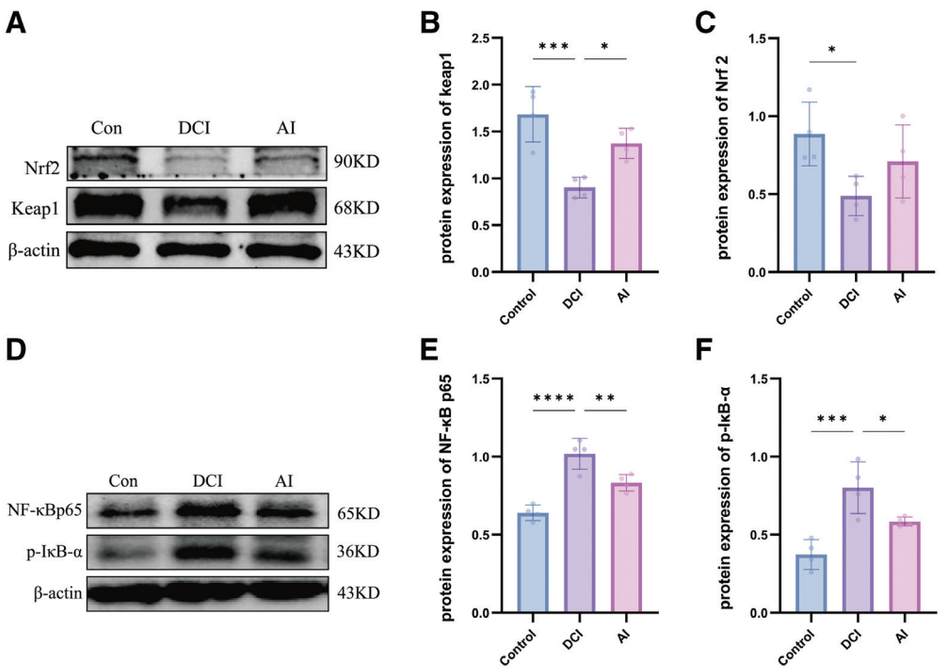


Figure 11. AI mitigates oxidative stress and inflammation in RBMECs. (A, D) Representative bands from western blot data; (B) quantitative analysis of Keap1 western blot bands; (C) quantitative analysis of Nrf2 western blot bands; (E) quantitative analysis of NF-κBp65 western blot bands; (F) quantitative analysis of p-IκB-α western blot bands; data were expressed as mean ± standard error. *$P < 0.05$, **$P < 0.01$, ***$P < 0.001$, ****$P < 0.0001$ compared to the DCI group. AI: Astragalus injection; DCI: Cognitive Impairment of Diabetes; Keap1: Kelch-like ECH-associated protein; NF-κB: Nuclear factor-kappa B; Nrf2: Nuclear factor-erythroid-derived related factor 2; RBMECs: Rat brain microvascular endothelial cells.

that AI may improve DCI through its potential to maintain blood-brain barrier integrity by coordinating both antioxidant and anti-inflammatory pathways.

Nrf2 is a prominent transcription factor that plays a crucial role in the regulation of redox-related genes. It exhibits a close relationship with Keap1 and forms complexes, participating in the process of regulating the expression of important antioxidant proteins, such as SOD and GSH-P. Consequently, the imbalance in redox molecular signal transduction mediated by the damaged Keap1/Nrf2 signaling pathway may be the potential pathogenesis of DCI. Numerous drug studies have been conducted to alleviate oxidative stress in mice and rats by regulating the Keap1/Nrf2 signaling pathway, verifying that it is an effective target and pathway for treating neurodegenerative diseases[34–35]. Our results show that AI can upregulate Nrf2 and Keap1 protein expression in the hippocampus of DCI rats, promote the nuclear translocation of Nrf2 in neurons, activate the Keap1/Nrf2 pathway to facilitate the release of downstream antioxidant mediators, and ultimately ameliorate oxidative stress resulting from T1DM. A deep-seated antagonistic relationship exists between the Nrf2 and NF-κB signaling pathways. Specifically, key antioxidant enzymes such as heme oxygenase-1, which are upregulated by Nrf2, and their metabolites can directly interfere with NF-κB signaling, thereby suppressing the expression of downstream pro-inflammatory cytokines[36].

NF-κB, an important regulator of inflammatory cell production, covalently binds to the inhibitor protein IκB in the cytoplasm. Stimulation of TLRs with their corresponding ligands can activate NF-κB by promoting the phosphorylation of IκB[37]. When activated, NF-κB translocates to the nucleus where it binds to specific target genes, initiating gene transcription and regulating inflammatory mediators expression, including pro-inflammatory factors TNF-α and IL-1β, as well as the anti-inflammatory factor IL-10[38]. Among them, NF-κBp65, as a member of the NF-κB family, its nuclear translocation is usually regarded as a marker of NF-κB activation, which plays a vital role in inflammation and acute immune response under various pathophysiological conditions[39]. Many studies have focused on inhibiting the TLR-4/NF-κB signaling pathway to treat inflammation in a variety of systems, including the nervous system[40–43]. We found that the TLR-4 and TNF-α expression in the hippocampus of the AI-M and AI-H group rats decreased significantly, p-IκB-α/IκB-α ratio decreased, and the content of NF-κBp65 decreased, which suggested that the activity of inflammatory signal pathway mediated by NF-κB was inhibited by AI. The p-IκB-α/IκB-α ratio in the AI-L group was not significantly lower than that in the DCI group, which was speculated to be related to its failure to reach the corresponding drug concentration. AI may reduce the release of inflammatory mediators by suppressing the TLR-4/NF-κB pathway, thereby improving neural function and attenuating the occurrence and development of DCI.

In conclusion, this study integrated network pharmacology and experimental validation to elucidate the potential mechanisms of AI in the treatment of DCI. However, limitations remain: first, the accuracy of database information may affect predictions, and the pharmacological effects of AI's active components have

HM9_V6N2.indb 244 25-Jun-26 00:45:18

not been validated individually. Regarding the cellular model, LPS-induced inflammation was used primarily to verify the direct anti-inflammatory effects of AI by activating explicit signaling pathways. Notably, this model mimics acute infection-related inflammation, which differs from the chronic low-grade inflammation in the diabetic microenvironment. Nonetheless, the shared downstream NF-κB signaling pathway supports the relevance of our findings. Further studies using models that better simulate metabolic inflammation are warranted. Additionally, the expression of Nrf2 downstream targets was not measured; thus, although Nrf2 nuclear translocation was confirmed, functional activation of the entire pathway requires further verification. Despite these limitations, our study provides foundational evidence for AI's activation of the Keap1/Nrf2 pathway and offers new insights into AI's potential as a therapeutic agent for DCI.

Conclusion

Our results indicated that AI can effectively alleviate hyperglycemia and improve cognitive impairment in T1DM rats with DCI. This compound may protect the BBB by alleviating oxidative stress and inflammation-induced damage to brain microvascular endothelial cells.

Conflict of interest statement

The authors declare no conflict of interest.

Funding

This study was supported by the National Natural Science Foundation of China (No. 81904146, 82004330), Tianjin Municipal Education Commission Research Project (No. 2023ZD024), Research project on the integrative medicine by the Tianjin Municipal Health Commission (No. 2023075), Tianjin Research Innovation Project for Postgraduate Students (No. 2022SKY238), Traditional Chinese medicine project of Jiangxi Provincial Health Commission (No. 2018A397).

Author contributions

Tong Xia contributed to validation, writing–original draft. Fayin Huang contributed to the investigation and methodology. Shiqi Li, Yijing Yan, Yijing Wang, Yanrong Suo, Maojuan Guo, and Xijuan Jiang contributed to the investigation. Lin Guo and Peizhe Lin contributed to data curation. Wenlan Zhang contributed to methodology, writing–review and editing. Yulin Wang contributed to methodology. Huhu Li and Yongna Dai contributed to conceptualization, funding acquisition, and supervision. Wenyun Zeng contributed to supervision. All data were generated in-house, and no paper mill was used. All authors agreed to be accountable for all aspects of work ensuring integrity and accuracy.

Ethical approval of studies and informed consent

The animal experiments were approved by the Ethics Committee of Tianjin University of Traditional Chinese Medicine (Animal Experiment Ethics No.: TCM-LAEC2023267X1634).

Acknowledgments

None.

Data availability

The datasets used or analyzed throughout this study are available from the corresponding author upon reasonable request.

Declaration of Generative AI in Scientific Writing

The authors used generative AI to assist with English language polishing, grammar correction, and improvement of readability. No generative AI was used for data analysis, interpretation of results, or drawing scientific conclusions. The authors reviewed and approved the final manuscript and take full responsibility for its content.

References

[1] Liu Z, Wang H, Yang Z, et al. Causal associations between type 1 diabetes mellitus and cardiovascular diseases: a Mendelian randomization study. *Cardiovasc Diabetol* 2023;22(1):236.
[2] Li W, Huang E, Gao S. Type 1 diabetes mellitus and cognitive impairments: a systematic review. *J Alzheimers Dis* 2017;57(1):29–36.
[3] Biessels GJ, Despa F. Cognitive decline and dementia in diabetes mellitus: mechanisms and clinical implications. *Nat Rev Endocrinol* 2018;14(10):591–604.
[4] Rawlings AM, Sharrett AR, Albert MS, et al. The association of late-life diabetes status and hyperglycemia with incident mild cognitive impairment and dementia: the ARIC study. *Diabetes Care* 2019;42(7):1248–1254.
[5] Roberts RO, Knopman DS, Geda YE, et al. Association of diabetes with amnestic and nonamnestic mild cognitive impairment. *Alzheimers Dement* 2014;10(1):18–26.
[6] Velayudhan L, Poppe M, Archer N, et al. Risk of developing dementia in people with diabetes and mild cognitive impairment. *Br J Psychiatry* 2010;196(1):36–40.
[7] Pickering J, Wong R, Al-Salami H, et al. Cognitive deficits in type-1 diabetes: aspects of glucose, cerebrovascular and amyloid involvement. *Pharm Res* 2021;38(9):1477–1484.
[8] Zhang BL, Dong ED, Liu L, et al. Ten recommendations for the high-quality development of traditional Chinese medicine in the new era. *Acupunct Herb Med* 2025;5(2):131–133.
[9] Pang B, Chen YB, Lyu HT, et al. Modern technological advances in traditional medicine: global insights from the 2025 top 50 high-impact researches. *Acupunct Herb Med* 2025;5(4):491–497.
[10] Cui K, Zhang S, Jiang X, et al. Novel synergic antidiabetic effects of Astragalus polysaccharides combined with Crataegus flavonoids *via* improvement of islet function and liver metabolism. *Mol Med Rep* 2016;13(6):4737–4744.
[11] Luo BY, Wang WT, Li YW, et al. Tetramethylpyrazine attenuates chronic intermittent hypoxia-exacerbated diabetic atherosclerosis: A mechanistic study of the IRE1α-XBP1 signaling pathway. *Acupunct Herb Med* 2025;5(2):160-172.
[12] Yue SJ, Liu J, Feng W-W, et al. System pharmacology-based dissection of the synergistic mechanism of Huangqi and Huanglian for diabetes mellitus. *Front Pharmacol* 2017;8:694.
[13] Zhang Y, Yuan Y, Zhang J, et al. Astragaloside IV supplementation attenuates cognitive impairment by inhibiting neuroinflammation and oxidative stress in type 2 diabetic mice. *Front Aging Neurosci* 2022;14:1004557.
[14] Wang X, Wang Y, Hu JP, et al. Astragaloside IV, a natural PPARgamma agonist, reduces a beta production in Alzheimer's disease through inhibition of BACE1. *Mol Neurobiol* 2017;54(4):2939–2949.
[15] Shang L, Wang Y, Li J, et al. Mechanism of Sijunzi Decoction in the treatment of colorectal cancer based on network pharmacology and experimental validation. *J Ethnopharmacol* 2023;302(Pt A):115876.

HM9_V6N2.indb 245 25-Jun-26 00:45:18

[16] Furman BL. Streptozotocin-induced diabetic models in mice and rats. *Curr Protoc* 2021;1(4):e78.
[17] Janhavi P, Divyashree S, Sanjailal KP, et al. DoseCal: a virtual calculator for dosage conversion between human and different animal species. *Arch Physiol Biochem* 2022;128(2):426–430.
[18] Vorhees CV, Williams MT. Morris water maze: procedures for assessing spatial and related forms of learning and memory. *Nat Protoc* 2006;1(2):848–858.
[19] Sun K, Ding M, Fu C, et al. Effects of dietary wild bitter melon (Momordica charantia var. abbreviate Ser.) extract on glucose and lipid metabolism in HFD/STZ-induced type 2 diabetic rats. *J Ethnopharmacol* 2023;306:116154.
[20] Li X, Gao Y, Li B, et al. Integrated proteomics and metabolomics analysis of D-pinitol function during hippocampal damage in streptozocin-induced aging-accelerated mice. *Front Mol Neurosci* 2023;16:1251513.
[21] Zhu X, Li N, Lv D, et al. Mechanism of Astragali Radix intervention in peritoneal fibrosis based on network pharmacology and molecular docking technology. *Drugs Clinic* 2022;37(4):700–707.
[22] Bettio L, Rajendran L, Gil-Mohapel J. The effects of aging in the hippocampus and cognitive decline. *Neurosci Biobehav Rev* 2017;79:66–86.
[23] Mehta BK, Banerjee S. Minocycline reverses diabetes-associated cognitive impairment in rats. *Pharmacol Rep* 2019;71(4):713–720.
[24] Liu YW, Zhu X, Zhang L, et al. Cerebroprotective effects of ibuprofen on diabetic encephalopathy in rats. *Pharmacol Biochem Behav* 2014;117:128–136.
[25] Hua Y, Xue W, Zhang M, et al. Metabonomics study on the hepatoprotective effect of polysaccharides from different preparations of Angelica sinensis. *J Ethnopharmacol* 2014;151(3):1090–1099.
[26] Liu DS, Zhou YH, Liang ES, et al. Neuroprotective effects of the Chinese Yi-Qi-Bu-Shen recipe extract on injury of rat hippocampal neurons induced by hypoxia/reoxygenation. *J Ethnopharmacol* 2013;145(1):168–174.
[27] Sancar G, Liu S, Gasser E, et al. FGF1 and insulin control lipolysis by convergent pathways. *Cell Metab* 2022;34(1):171–183.e6.
[28] Zhang Y, Gu Y, Ren H, et al. Gut microbiome-related effects of berberine and probiotics on type 2 diabetes (the PREMOTE study). *Nat Commun* 2020;11(1):5015.
[29] Albazal A, Delshad AA, Roghani M. Melatonin reverses cognitive deficits in streptozotocin-induced type 1 diabetes in the rat through attenuation of oxidative stress and inflammation. *J Chem Neuroanat* 2021;112:101902.
[30] Xiang X, Wang X, Wu YM, et al. Activation of GPR55 attenuates cognitive impairment, oxidative stress, neuroinflammation, and synaptic dysfunction in a streptozotocin-induced Alzheimer's mouse model. *Pharmacol Biochem Behav* 2022;214:173340.
[31] Vittal RH, Waseem SB, Iannucci J, et al. Thrombin signaling contributes to high glucose-induced injury of human brain microvascular endothelial cells. *J Alzheimers Dis* 2021;79(1):211–224.
[32] Zhang Z, Yang H, Yang J, et al. Pseudoginsenoside-F11 attenuates cognitive impairment by ameliorating oxidative stress and neuroinflammation in d-galactose-treated mice. *Int Immunopharmacol* 2019;67:78–86.
[33] Piatkowska-Chmiel I, Herbet M, Gawronska-Grzywacz M, et al. The role of molecular and inflammatory indicators in the assessment of cognitive dysfunction in a mouse model of diabetes. *Int J Mol Sci* 2021;22(8):3878.
[34] Sun Y, Huang J, Chen Y, et al. Direct inhibition of Keap1-Nrf2 Protein-Protein interaction as a potential therapeutic strategy for Alzheimer's disease. *Bioorg Chem* 2020;103:104172.
[35] Medhat E, Rashed L, Abdelgwad M, et al. Exercise enhances the effectiveness of vitamin D therapy in rats with Alzheimer's disease: emphasis on oxidative stress and inflammation. *Metab Brain Dis* 2020;35(1):111–120.
[36] Wardyn JD, Ponsford AH, Sanderson CM. Dissecting molecular cross-talk between Nrf2 and NF-κB response pathways. *Biochem Soc Trans* 2015;43(4):621–626.
[37] Wang T, Zhang X, Li JJ. The role of NF-kappaB in the regulation of cell stress responses. *Int Immunopharmacol* 2002;2(11):1509–1520.
[38] Shi Y, Tu Z, Tang D, et al. The inhibition of LPS-induced production of inflammatory cytokines by HSP70 involves inactivation of the NF-kappaB pathway but not the MAPK pathways. *Shock* 2006;26(3):277–284.
[39] Liu Y, Wu H, Nie Y-C, et al. Naringin attenuates acute lung injury in LPS-treated mice by inhibiting NF-kappaB pathway. *Int Immunopharmacol* 2011;11(10):1606–1612.
[40] Khayatan D, Razavi SM, Arab ZN, et al. Protective effects of curcumin against traumatic brain injury. *Biomed Pharmacother* 2022;154:113621.
[41] Xiong T, Zheng X, Zhang K, et al. Ganluyin ameliorates DSS-induced ulcerative colitis by inhibiting the enteric-origin LPS/TLR4/NF-kappaB pathway. *J Ethnopharmacol* 2022;289:115001.
[42] Wang YM, Ji R, Chen W-W, et al. Paclitaxel alleviated sepsis-induced acute lung injury by activating MUC1 and suppressing TLR-4/NF-kappaB pathway. *Drug Des Devel Ther* 2019;13:3391–3404.
[43] Abdel Baky NA, Al-Najjar AH, Elariny HA, et al. Pramipexole and lactoferrin ameliorate cyclophosphamide-induced haemorrhagic cystitis *via* targeting Sphk1/S1P/MAPK, TLR-4/NF-kappaB, and NLRP3/caspase-1/IL-1beta signalling pathways and modulating the Nrf2/HO-1 pathway. *Int Immunopharmacol* 2022;112:109282.

HM9_V6N2.indb 246 25-Jun-26 00:45:18